We are IntechOpen,
the world's leading publisher of
Open Access books
Built by scientists, for scientists

4,800
Open access books available

122,000
International authors and editors

135M
Downloads

Our authors are among the

154
Countries delivered to

TOP 1%
most cited scientists

12.2%
Contributors from top 500 universities

CLARIVATE ANALYTICS

BOOK CITATION INDEX

INDEXED

WEB OF SCIENCE™

Selection of our books indexed in the Book Citation Index
in Web of Science™ Core Collection (BKCI)

Interested in publishing with us?
Contact book.department@intechopen.com

Numbers displayed above are based on latest data collected.
For more information visit www.intechopen.com

Advanced Humanoid Robot Based on the Evolutionary Inductive Self-organizing Network

Dongwon Kim, and Gwi-Tae Park

Department of Electrical Engineering, Korea University,
1, 5-ka, Anam-dong, Seongbuk-ku, Seoul 136-701,
Korea.

1. Introduction

The bipedal structure is one of the most versatile ones for the employment of walking robots. The biped robot has almost the same mechanisms as a human and is suitable for moving in an environment which contains stairs, obstacle etc, where a human lives. However, the dynamics involved are highly nonlinear, complex and unstable. So it is difficult to generate human-like walking motion. To realize human-shaped and human-like walking robots, we call this as *humanoid robot*, many researches on the biped walking robots have been reported [1-4]. In contrast to industrial robot manipulators, the interaction between the walking robots and the ground is complex. The concept of the zero moment point (ZMP) [2] is known to give good results in order to control this interaction. As an important criterion for the stability of the walk, the trajectory of the ZMP beneath the robot foot during the walk is investigated [1-7]. Through the ZMP, we can synthesize the walking patterns of humanoid robot and demonstrate walking motion with real robots. Thus ZMP is indispensable to ensure dynamic stability for a biped robot. The ZMP represents the point at which the ground reaction force is applied. The location of the ZMP can be obtained computationally using a model of the robot. But it is possible that there is a large error between the actual ZMP and the calculated one, due to the deviations of the physical parameters between the mathematical model and the real machine. Thus, actual ZMP should be measured to realize stable walking with a control method that makes use of it.

In this chapter, actual ZMP data throughout the whole walking phase are obtained from the practical humanoid robot. And evolutionary inductive self-organizing network [8-9] is applied. So we obtained natural walking motions on the flat floor, some slopes, and uneven floor.

2. Evolutionary Inductive Self-organizing Network

In this Section we will depict the evolutionary inductive self-organizing network (EISON) to be applied to the practical humanoid robot. Firstly the algorithm and its structure are shown and evaluation to show the usefulness of the method will be followed.

2.1 Algorithm and structure

The EISON has an architecture similar to feed-forward neural networks whose neurons are replaced by polynomial nodes. The output of the each node in EISON structure is obtained using several types of high-order polynomial such as linear, quadratic, and modified quadratic of input variables. These polynomials are called as partial descriptions (PDs). The PDs in each layer can be designed by evolutionary algorithm. The framework of the design procedure of the EISON [8-9] comes as a sequence of the following steps.

[Step 1] *Determine input candidates of a system to be targeted.*
[Step 2] *Form training and testing data.*
[Step 3] *Design partial descriptions and structure evolutionally.*
[Step 4] *Check the stopping criterion.*
[Step 5] *Determine new input variables for the next layer.*

In the following, a more in-depth discussion on the design procedures, step 1~step 5, is provided.

Step 1: *Determine input candidates of a system to be targeted*
We define the input variables such as $x_{1i}, x_{2i}, \cdots x_{Ni}$ related to output variables y_i, where N and i are the number of entire input variables and input-output data set, respectively.

Step 2: *Form training and testing data.*
The input - output data set is separated into training (n_{tr}) data set and testing (n_{te}) data set. Obviously we have $n = n_{tr} + n_{te}$. The training data set is used to construct a EISON model. And the testing data set is used to evaluate the constructed EISON model.

Step 3: *Design partial descriptions(PD) and structure evolutionally.*
When we design the EISON, the most important consideration is the representation strategy, that is, how to encode the key factors of the PDs, order of the polynomial, the number of input variables, and the optimum input variables, into the chromosome. We employ a binary coding for the available design specifications. We code the order and the inputs of each node in the EISON as a finite-length string. Our chromosomes are made of three sub-chromosomes. The first one is consisted of 2 bits for the order of polynomial (PD), the second one is consisted of 3 bits for the number of inputs of PD, and the last one is consisted of N bits which are equal to the number of entire input candidates in the current layer. These input candidates are the node outputs of the previous layer. The representation of binary chromosomes is illustrated in Fig. 1.

Bits in the 1st sub-chromosome	Order of polynomial(PD)
00	Type 1 – Linear
01	Type 2 – Quadratic
10	
11	Type 3 – Modified quadratic

Table 1. Relationship between bits in the 1st sub-chromosome and order of PD.

The 1st sub-chromosome is made of 2 bits. It represents several types of order of PD. The relationship between bits in the 1st sub-chromosome and the order of PD is shown in Table 1. Thus, each node can exploit a different order of the polynomial.
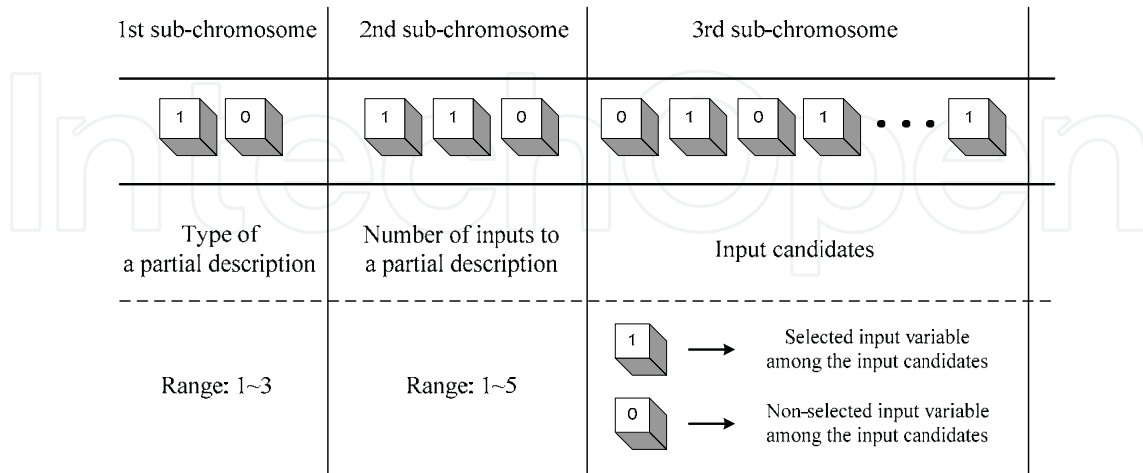
Fig. 1. Structure of binary chromosome for a PD

The 3rd sub-chromosome has N bits, which are concatenated a bit of 0's and 1's coding. The input candidate is represented by a 1 bit if it is chosen as input variable to the PD and by a 0 bit it is not chosen. This way solves the problem of which input variables to be chosen.

If many input candidates are chosen for model design, the modeling is computationally complex, and normally requires a lot of time to achieve good results. In addition, it causes improper results and poor generalization ability. Good approximation performance does not necessarily guarantee good generalization capability. To overcome this drawback, we introduce the 2nd sub-chromosome into the chromosome. The 2nd sub-chromosome is consisted of 3 bits and represents the number of input variables to be selected. The number based on the 2nd sub-chromosome is shown in the Table 2.

Bits in the 2nd sub-chromosome	Number of inputs to PD
000	1
001	2
010	2
011	3
100	3
101	4
110	4
111	5

Table 2. Relationship between bits in the 2nd sub-chromosome and number of inputs to PD.

Input variables for each node are selected among entire input candidates as many as the number represented in the 2nd sub-chromosome. Designer must determine the maximum number in consideration of the characteristic of system, design specification, and some prior knowledge of model. With this method we can solve the problems such as the conflict between overfitting and generalization and the requirement of a lot of computing time.

The relationship between chromosome and information on PD is shown in Fig. 2. The PD corresponding to the chromosome in Fig. 2 is described briefly as Fig. 3.

Fig. 2 shows an example of PD. The various pieces of required information are obtained its chromosome. The 1st sub-chromosome shows that the polynomial order is Type 2 (quadratic form). The 2nd sub-chromosome shows two input variables to this node. The 3rd sub-chromosome tells that x_1 and x_6 are selected as input variables. The node with PD corresponding to Fig. 2 is shown in Fig. 3. Thus, the output of this PD, $\hat{y}$ can be expressed as (1).

$$\hat{y} = f(x_1, x_6) = c_0 + c_1 x_1 + c_2 x_6 + c_3 x_1^2 + c_4 x_6^2 + c_5 x_1 x_6 \tag{1}$$

where coefficients c_0, c_1, …, c_5 are evaluated using the training data set by means of the standard least square estimation (LSE). Therefore, the polynomial function of PD is formed automatically according to the information of sub-chromosomes.
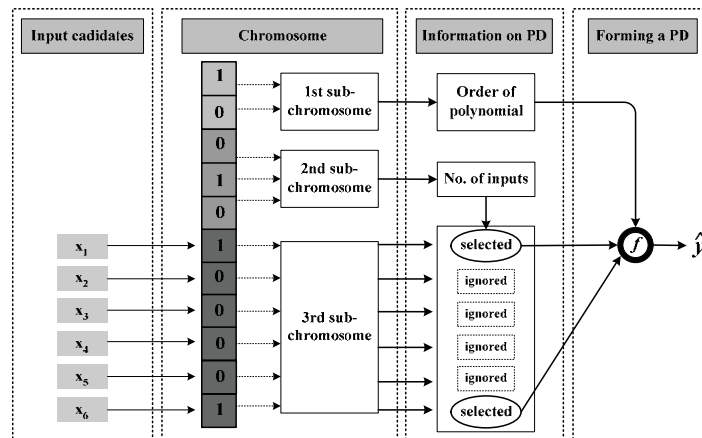

Fig. 2. Example of PD whose various pieces of required information are obtained from its chromosome.
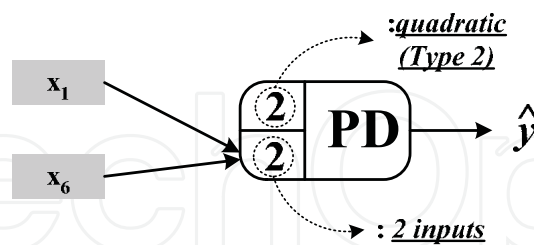

Fig. 3. Node with PD corresponding to chromosome in Fig. 2.

Step 4: *Check the stopping criterion.*
The EISON algorithm terminates when the 3rd layer is reached.

Step 5: *Determine new input variables for the next layer.*
If the stopping criterion is not satisfied, the next layer is constructed by repeating step 3 through step 4.
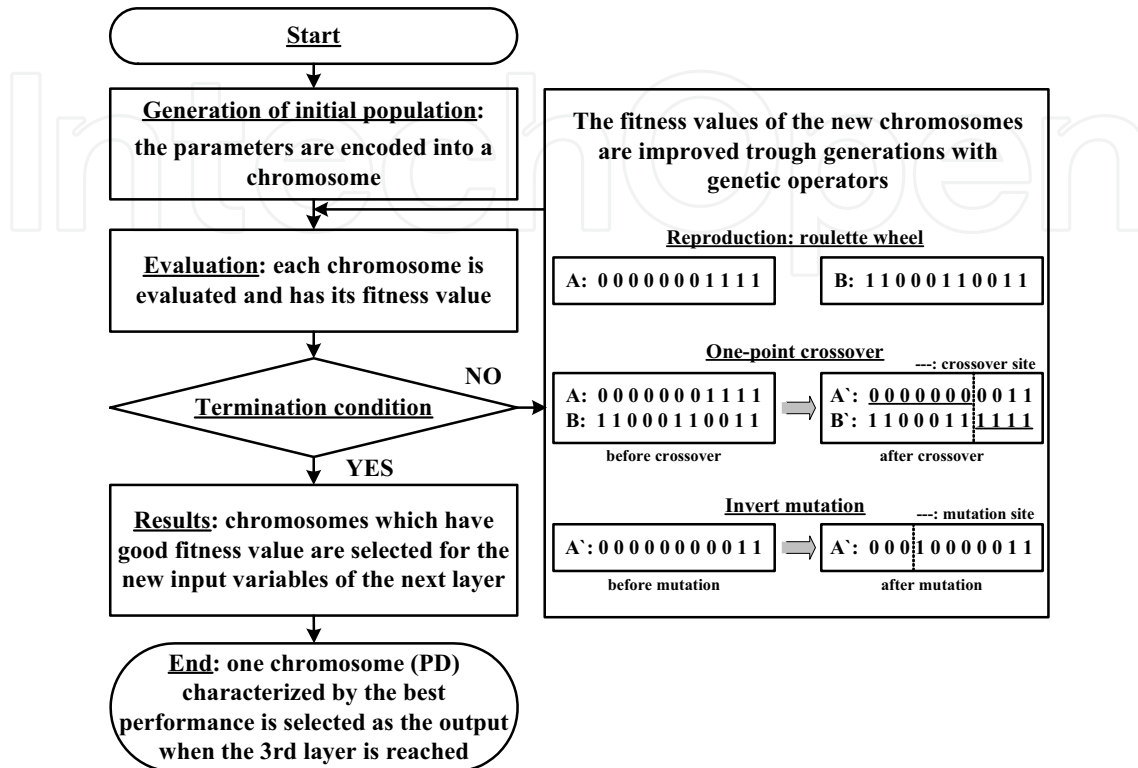
Fig. 4. Block diagram of the design procedure of EISON.

The overall design procedure of EISON is shown in Fig. 4. At the beginning of the process, the initial populations comprise a set of chromosomes that are scattered all over the search space. The populations are all randomly initialized. Thus, the use of heuristic knowledge is minimized. The assignment of the fitness in evolutionary algorithm serves as guidance to lead the search toward the optimal solution. Fitness function with several specific cases for modeling will be explained later. After each of the chromosomes is evaluated and associated with a fitness, the current population undergoes the reproduction process to create the next generation of population. The roulette-wheel selection scheme is used to determine the members of the new generation of population. After the new group of population is built, the mating pool is formed and the crossover is carried out. The crossover proceeds in three steps. First, two newly reproduced strings are selected from the mating pool produced by reproduction. Second, a position (one point) along the two strings is selected uniformly at random. The third step is to exchange all characters following the crossing site. We use one-point crossover operator with a crossover probability of P_c (0.85). This is then followed by the mutation operation. The mutation is the occasional alteration of a value at a particular bit position (we flip the states of a bit from 0 to 1 or vice versa). The mutation serves as an insurance policy which would recover the loss of a particular piece of information (any simple bit). The mutation rate used is fixed at 0.05 (P_m). Generally, after these three operations, the overall fitness of the population improves. Each of the population generated then goes through a series of evaluation, reproduction, crossover, and mutation, and the

procedure is repeated until a termination condition is reached. After the evolution process, the final generation of population consists of highly fit bits that provide optimal solutions. After the termination condition is satisfied, one chromosome (PD) with the best performance in the final generation of population is selected as the output PD. All remaining other chromosomes are discarded and all the nodes that do not have influence on this output PD in the previous layers are also removed. By doing this, the EISON model is obtained.

2.2 Fitness function for EISON

The important thing to be considered for the evolutionary algorithm is the determination of the fitness function. The genotype representation encodes the problem into a string while the fitness function measures the performance of the model. It is quite important for evolving systems to find a good fitness measurement. To construct models with significant approximation and generalization ability, we introduce the error function such as

$$E = \theta \times PI + (1-\theta) \times EPI \tag{2}$$

where $\theta \in [0,1]$ is a weighting factor for PI and EPI, which denote the values of the performance index for the training data and testing data, respectively, as expressed in (5). Then the fitness value is determined as follows:

$$F = \frac{1}{1+E} \tag{3}$$

Maximizing F is identical to minimizing E. The choice of θ establishes a certain tradeoff between the approximation and generalization ability of the EISON.

2.3 Evaluation of the EISON

We show the performance of our EISON for well known nonlinear system to see the applicability. In addition, we demonstrate how the proposed EISON model can be employed to identify the highly nonlinear function. The performance of this model will be compared with that of earlier works. The function to be identified is a three-input nonlinear function given by (4)

$$y = (1 + x_1^{0.5} + x_2^{-1} + x_3^{-1.5})^2 \tag{4}$$

which is widely used by Takagi and Hayashi [10], Sugeno and Kang[11], and Kondo[12] to test their modeling approaches.

40 pairs of the input-output data sets are obtained from (4) [14]. The data is divided into training data set (Nos. 1-20) and testing data set (Nos. 21-40). To compare the performance, the same performance index, average percentage error (APE) adopted in [10-14] is used.

$$APE = \frac{1}{m} \sum_{i=1}^{m} \frac{|y_i - \hat{y}_i|}{y_i} \times 100 \qquad (\%) \tag{5}$$

where m is the number of data pairs and y_i and $\hat{y}_i$ are the i-th actual output and model output, respectively.

The design parameters of EISON in each layer are shown in Table 3. The simulation results of the EISON are summarized in Table 4. The overall lowest values of the performance index, PI=0.188 EPI=1.087, are obtained at the third layer when the weighting factor (θ) is 0.25.

Parameters	1st layer	2nd layer	3rd layer
Maximum generations	40	60	80
Population size:(w)	20:(15)	60:(50)	80
String length	8	20	55
Crossover rate (P_c)	0.85		
Mutation rate (P_m)	0.05		
Weighting factor: θ	0.1~0.9		
Type (order)	1~3		

Table 3. Design parameters of EISON for modeling.

w: the number of chosen nodes whose outputs are used as inputs to the next layer

Weighting factor	1st layer		2nd layer		3rd layer	
	PI	EPI	PI	EPI	PI	EPI
0.1	5.7845	6.8199	2.3895	3.3400	2.2837	3.1418
0.25	5.7845	6.8199	0.8535	3.1356	0.1881	1.0879
0.5	5.7845	6.8199	1.6324	5.5291	1.2268	3.5526
0.75	5.7845	6.8199	1.9092	4.0896	0.5634	2.2097
0.9	5.7845	6.8199	2.5083	5.1444	0.0002	4.8804

Table 4. Values of performance index of the proposed EISON model.

(a) training result   (b) testing result
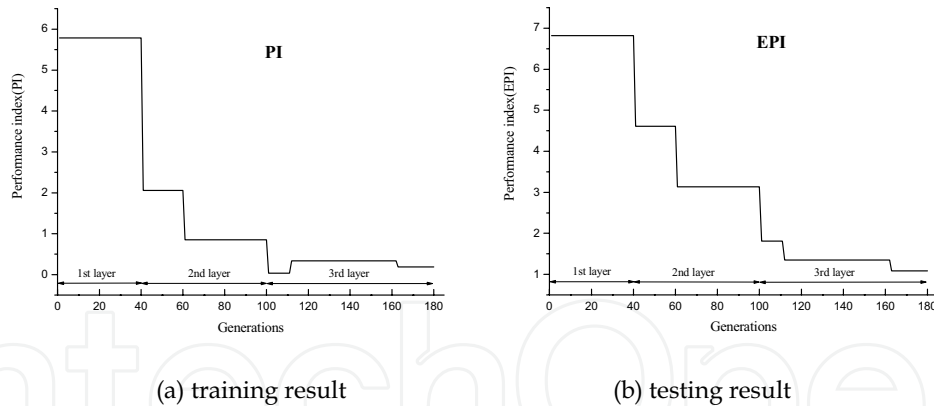
Fig. 5. Trend of performance index values with respect to generations through layers (θ =0.25).

Fig. 5 illustrates the trend of the performance index values produced in successive generations of the evolutionary algorithm when the weighting factor θ is 0.25. Fig. 6 shows the values of error function and fitness function in successive evolutionary algorithm generations when the θ is 0.25. Fig. 7 depicts the proposed EISON model with 3 layers when the θ is 0.25. The structure of EISON is very simple and has a good performance.
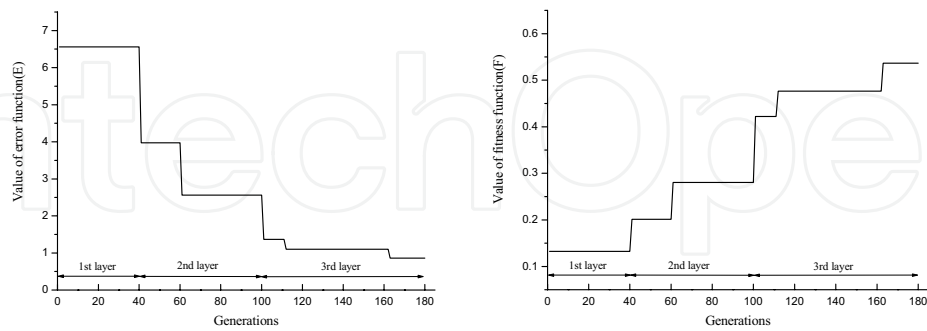
(a) error function (E)   (b) fitness function (F)

Fig. 6. Values of the error function and fitness function with respect to the successive generations (θ =0.25).
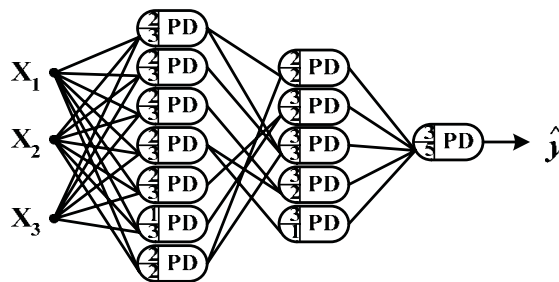

Fig. 7. Structure of the EISON model with 3 layers (θ =0.25).

Fig. 8 shows the identification performance of the proposed EISON and its errors when the θ is 0.25. The output of the EISON follows the actual output very well.

Table 5 shows the performance of the proposed EISON model and other models studied in the literature. The experimental results clearly show that the proposed model outperforms the existing models both in terms of better approximation capabilities (PI) as well as superb generalization abilities (EPI).

Model		APE	
		PI (%)	EPI (%)
GMDH model[12]		4.7	5.7
Fuzzy model [11]	Model 1	1.5	2.1
	Model 2	0.59	3.4
FNN [14]	Type 1	0.84	1.22
	Type 2	0.73	1.28
	Type 3	0.63	1.25
GD-FNN [13]		2.11	1.54
EISON		0.188	1.087

Table 5. Performance comparison of various identification models.
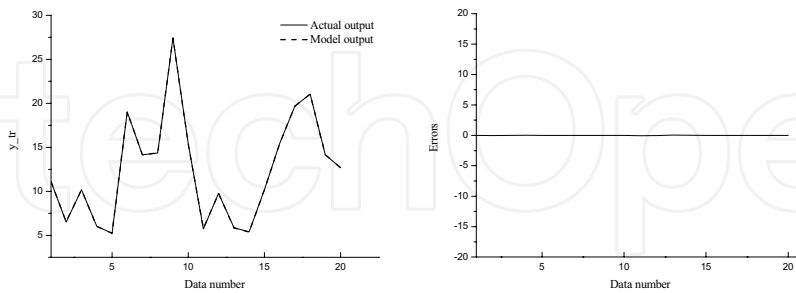
(a) actual versus model output of training data set   (b) errors of (a)
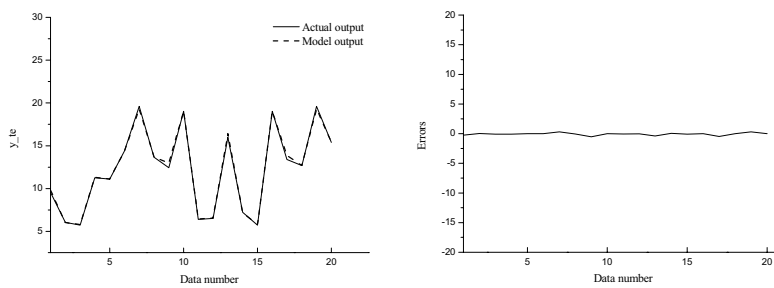
(c) actual versus model output of testing data set   (d) errors of (c)

Fig. 8. Identification performance of EISON model with 3 layers and its errors

3. Practical Biped Humanoid Robot

3.1 Design

Biped humanoid robot designed and implemented is shown in Fig. 9. The specification of our biped humanoid robot is depicted in Table 6. The robot has 19 joints and the height and the weight are about 445mm and 3000g including vision camera. For the reduction of the weight, the body is made of aluminum materials. Each joint is driven by the RC servomotor that consists of a DC motor, gear, and simple controller. Each of the RC servomotors is mounted in the link structure. This structure is strong against falling down of the robot and it looks smart and more similar to a human.

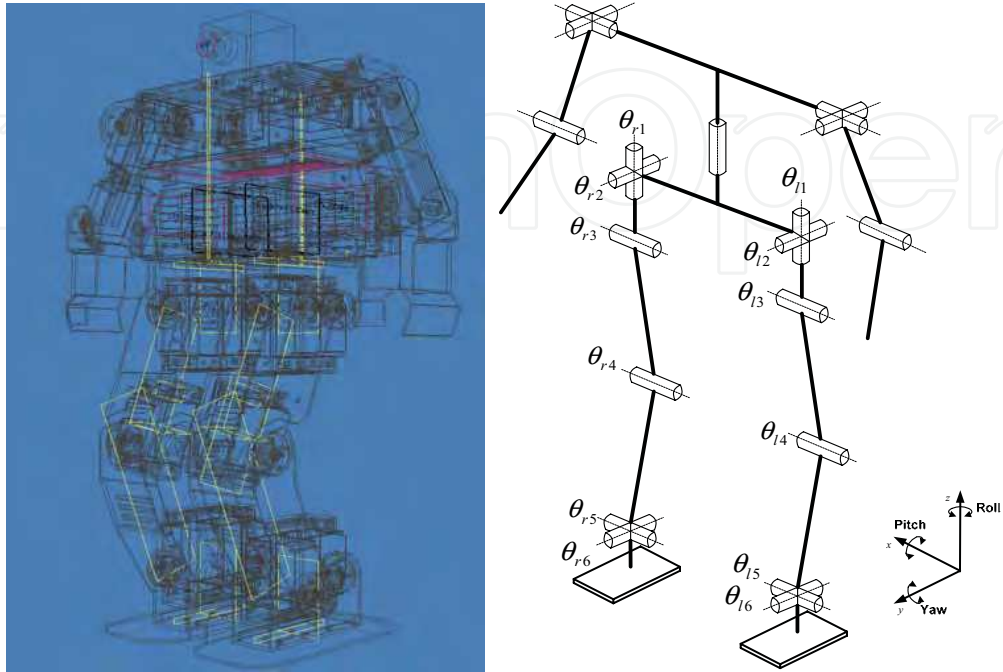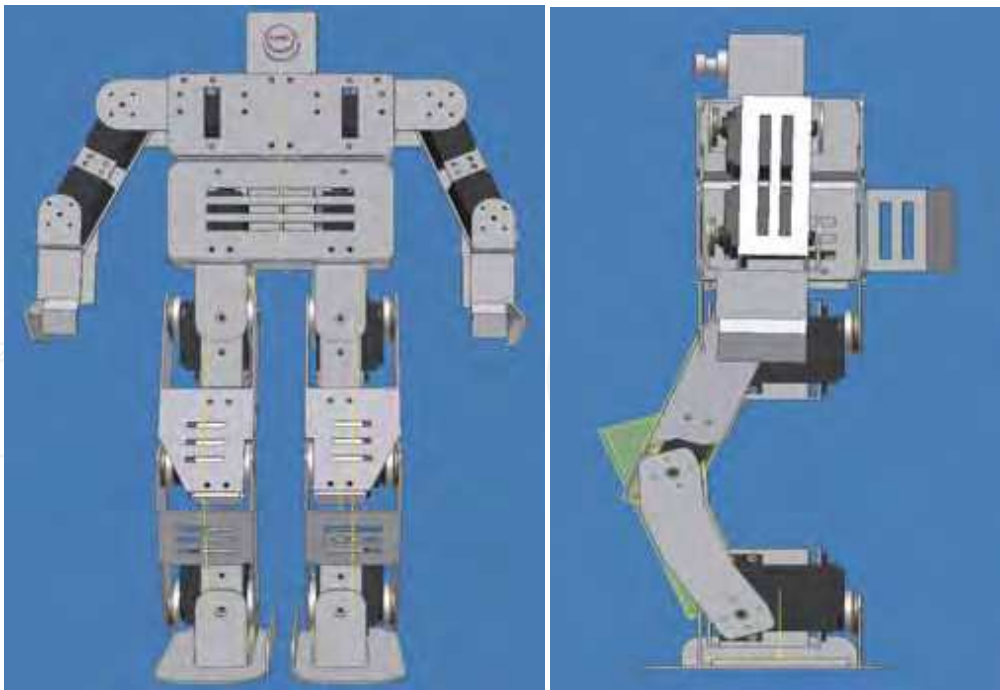| Size	Height : 445mm
Weight	3kg
CPU	TMS320LF2407 DSP
Actuator (RC Servo motors)	HSR-5995TG (Torque : 30kg·cm at 7.4V)
Degree of freedom	19 DOF (Leg+Arm+Waist) = 2*6 + 3*2+1)
Power source	Battery
Actuator	: AA Size Ni-poly (7.4V, 1700mAh)
Control board	: AAA size Ni- poly (7.4V, 700mAh)

Table 6. Specification of our humanoid robot

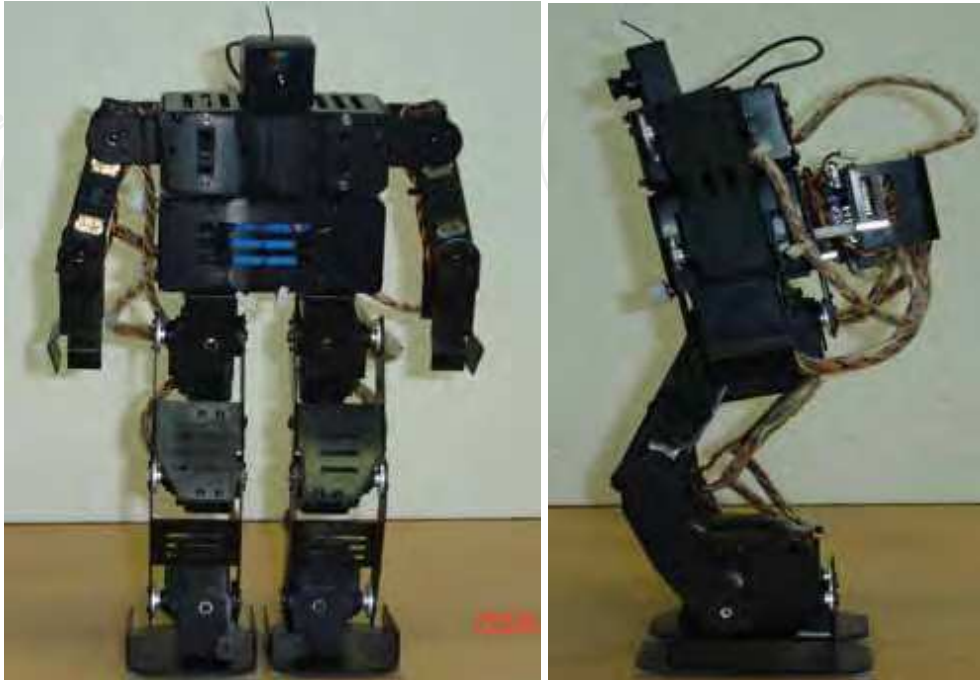Fig. 9. Designed and implemented humanoid robot.

Fig. 10. 3D humanoid robot design and its practical figures

Front and side view of 3D robot and its practical figures are shown in Fig. 10. Block diagram of the biped walking robot and its electric diagram of control board and actuators are also shown in Figs. 11 and 12, respectively. Implemented control board and its electric wiring diagram schematic is presented in Fig. 13.
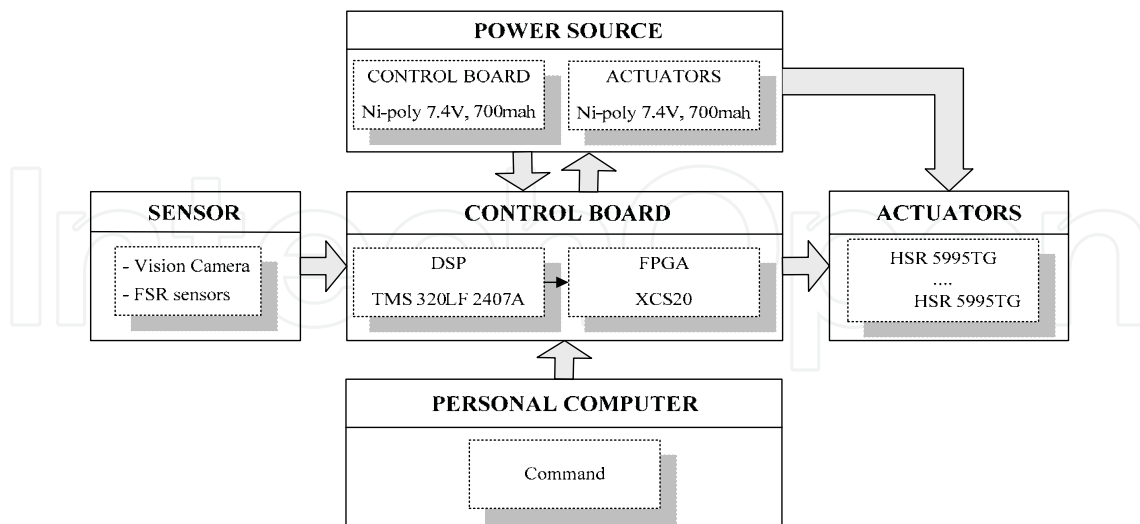

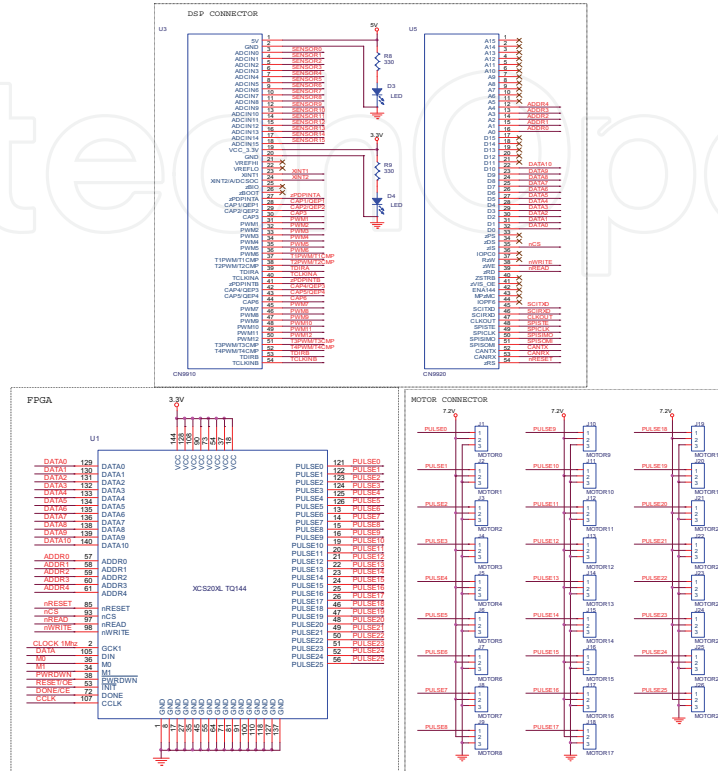Fig. 11. Block diagram of the humanoid robot

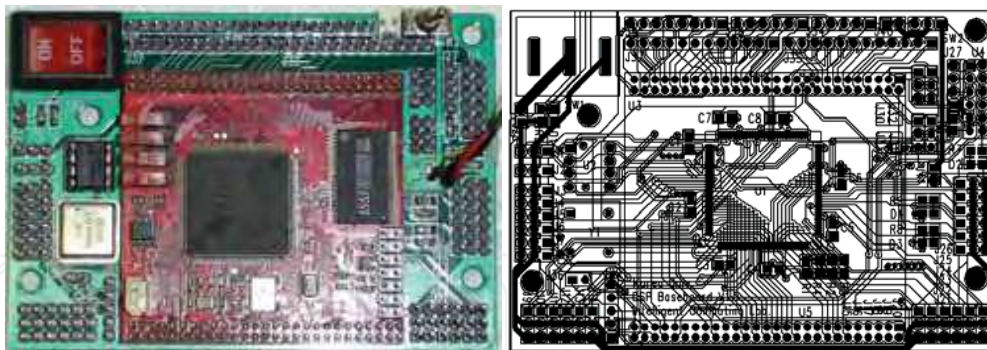Fig. 12. Electric diagram of control board and actuators

Fig. 13. Implemented control board and its electric wiring diagram schematic

3.2 Zero moment point measurement system

As an important criterion for the stability of the walk, the trajectory of the zero moment point (ZMP) beneath the robot foot during the walk is investigated. Through the ZMP, we can synthesize the walking patterns of biped walking robot and demonstrate walking motion with real robots. Thus ZMP is indispensable to ensure dynamic stability for a biped robot.
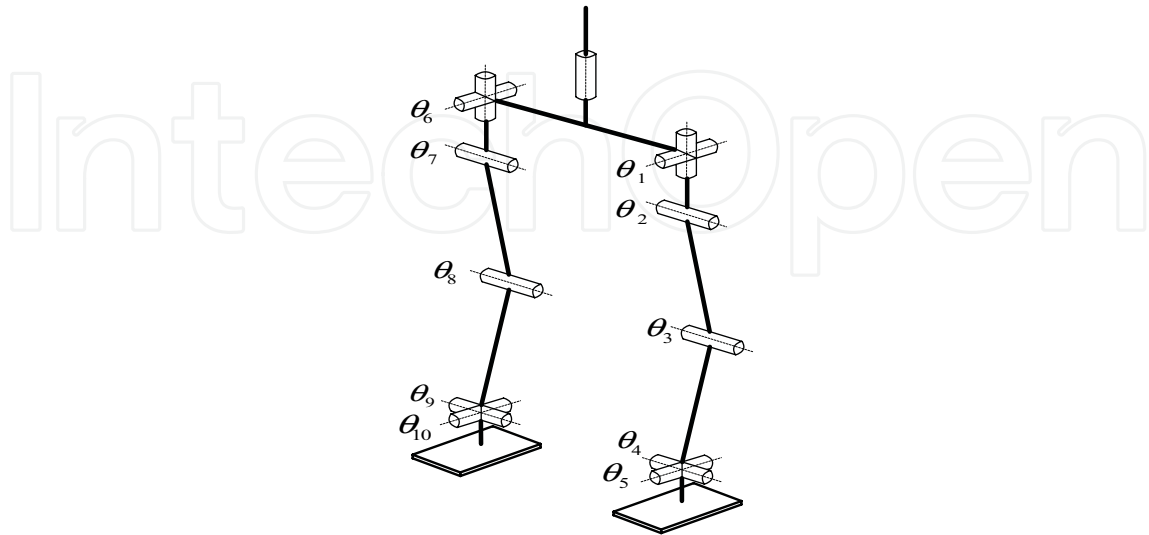
Fig. 14. Representation of joint angle of the 10 degree of freedoms.

The places of joints in walking are shown in Fig. 14. The measured ZMP trajectory data to be considered here are obtained from 10 degree of freedoms (DOFs) as shown in Fig. 14. Two DOFs are assigned to hips and ankles and one DOF to the knee on both sides. From these joint angles, cyclic walking pattern has been realized. This biped walking robot can walk continuously without falling down. The zero moment point (ZMP) trajectory in the robot foot support area is a significant criterion for the stability of the walk. In many studies, ZMP coordinates are computed using a model of the robot and information from the joint encoders. But we employed more direct approach which is to use measurement data from sensors mounted at the robot feet.

The type of force sensor used in our experiments is FlexiForce sensor A201 which is shown in Fig. 15. They are attached to the four corners of the sole plate. Sensor signals are digitized by an ADC board, with a sampling time of 10 ms. Measurements are carried out in real time.
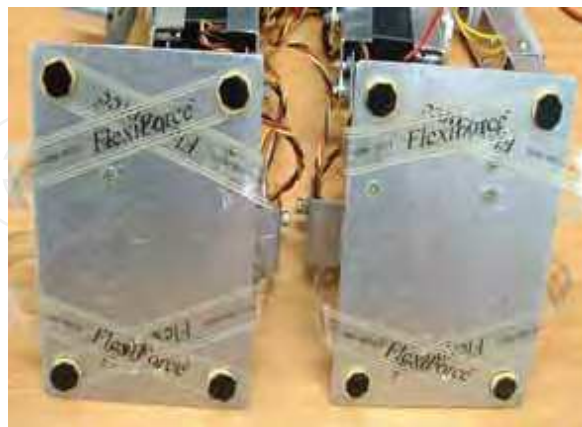

Fig. 15. Employed force sensors under the robot feet.

The foot pressure is obtained by summing the force signals. By using the force sensor data, it is easy to calculate the actual ZMP data. Feet support phase ZMPs in the local foot coordinate frame are computed by equation 6

$$P = \frac{\sum_{i=1}^{8} f_i r_i}{\sum_{i=1}^{8} f_i} \tag{6}$$

where f_i is each force applied to the right and left foot sensors and r_i is sensor position which is vector.

4. Walking Pattern Analysis of the Humanoid Robot

The walking motions of the biped humanoid robot are shown in Figs. 16-18. These figures show series of snapshots in the front views of the biped humanoid robot walking on a flat floor, some slopes, and uneven floor, respectively. Fig. 16 gives the series of front views of this humanoid robot walking on a flat floor. In Fig. 17 depict the series of front views of this humanoid robot going up on an ascent. Fig. 18 shows another type of walking of biped humanoid robot, which is walking motion on an uneven floor.

Fig. 16. Side view of the biped humanoid robot on a flat floor

Fig. 17. Side view of the biped humanoid robot on an ascent.

Fig. 18. Side view of the biped humanoid robot on an uneven floor.

Experiments using EISON was conducted and the results are summarized in tables and figures below. The design parameters of evolutionary inductive self-organizing network in each layer are shown in Table 7. The results of the EISON for the walking humanoid robot on the flat floor are summarized in Table 8. The overall lowest values of the performance indicies, 6.865 and 10.377, are obtained at the third layer when the weighting factor (θ) is 1. In addition, the generated ZMP positions and corresponding ZMP trajectory are shown in Fig. 19. Table 9 depicts the condition and results for the actual ZMP positions of our humanoid walking robot on an ascent floor. We can also see the corresponding ZMP trajectories in Fig. 20, respectively.

Parameters	1st layer	2nd layer	3rd layer
Maximum generations	40	60	80
Population size:(w)	40:(30)	100:(80)	160
String length	13	35	85
Crossover rate (P_c)	0.85		
Mutation rate (P_m)	0.05		
Weighting factor: θ	1		
Type (order)	1~3		

Table 7. Design parameters of evolutionary inductive self-organizing network.

w: the number of chosen nodes whose outputs are used as inputs to the next layer

Walking condition	Layer	MSE (mm)	
slope (deg.)		x-coordinate	y-coordinate
	1	9.676	18.566
0°	2	7.641	13.397
	3	6.865	10.377

Table 8. Condition and the corresponding MSE are included for actual ZMP position in four step motion of our humanoid robot.
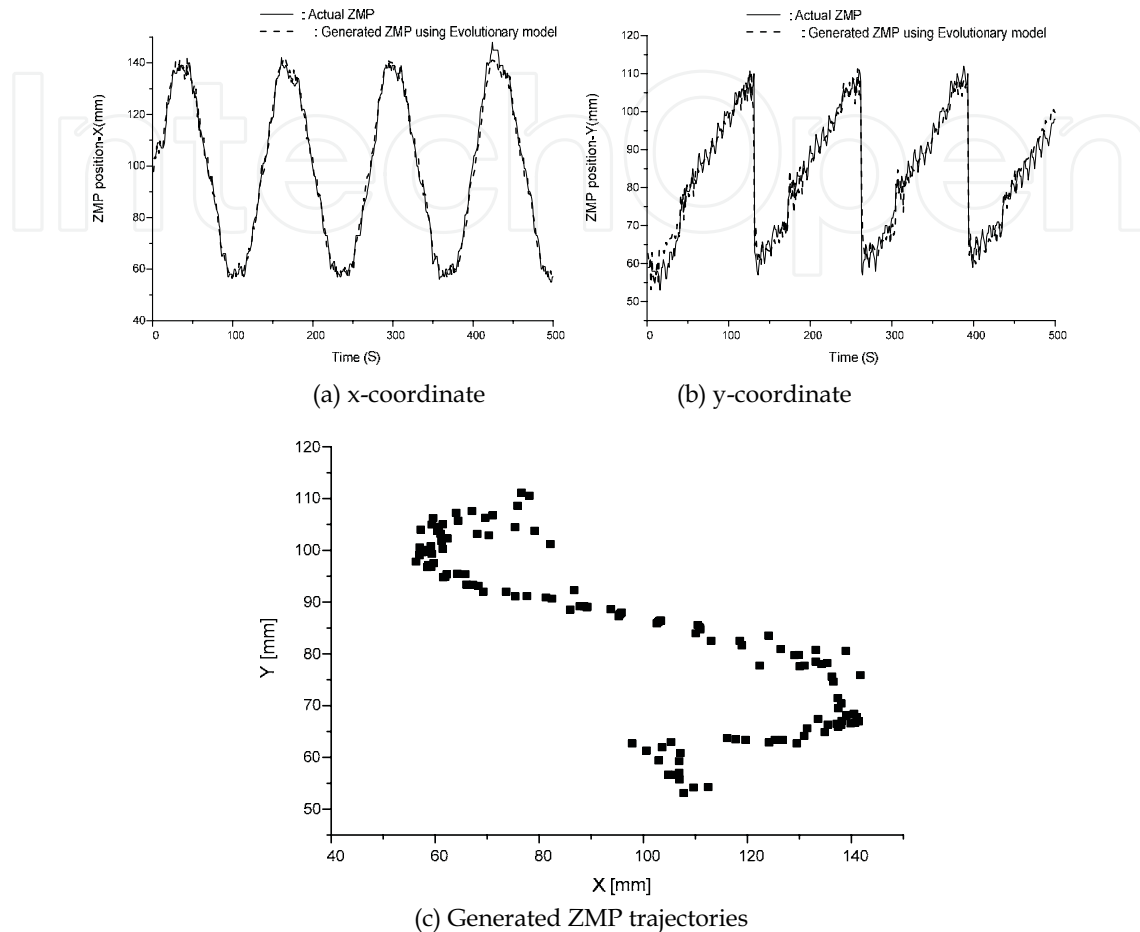
(a) x-coordinate   (b) y-coordinate

(c) Generated ZMP trajectories

Fig. 19. Generated ZMP positions and corresponding ZMP trajectories (0°).

5. Concluding remarks

This chapter deals with advanced humanoid robot based on the evolutionary inductive self-organizing network. Humanoid robot is the most versatile ones and has almost the same mechanisms as a human and is suitable for moving in an human's environment. But the dynamics involved are highly nonlinear, complex and unstable. So it is difficult to generate human-like walking motion. In this chapter, we have employed zero moment point as an important criterion for the balance of the walking robots. In addition, evolutionary inductive self-organizing network is also utilized to establish empirical relationships between the humanoid walking robots and the ground and to explain empirical laws by incorporating them into the humanoid robot. From obtained natural walking motions of the humanoid robot, EISON can be effectively used to the walking robot and we can see the synergy effect humanoid robot and evolutionary inductive self-organizing network.
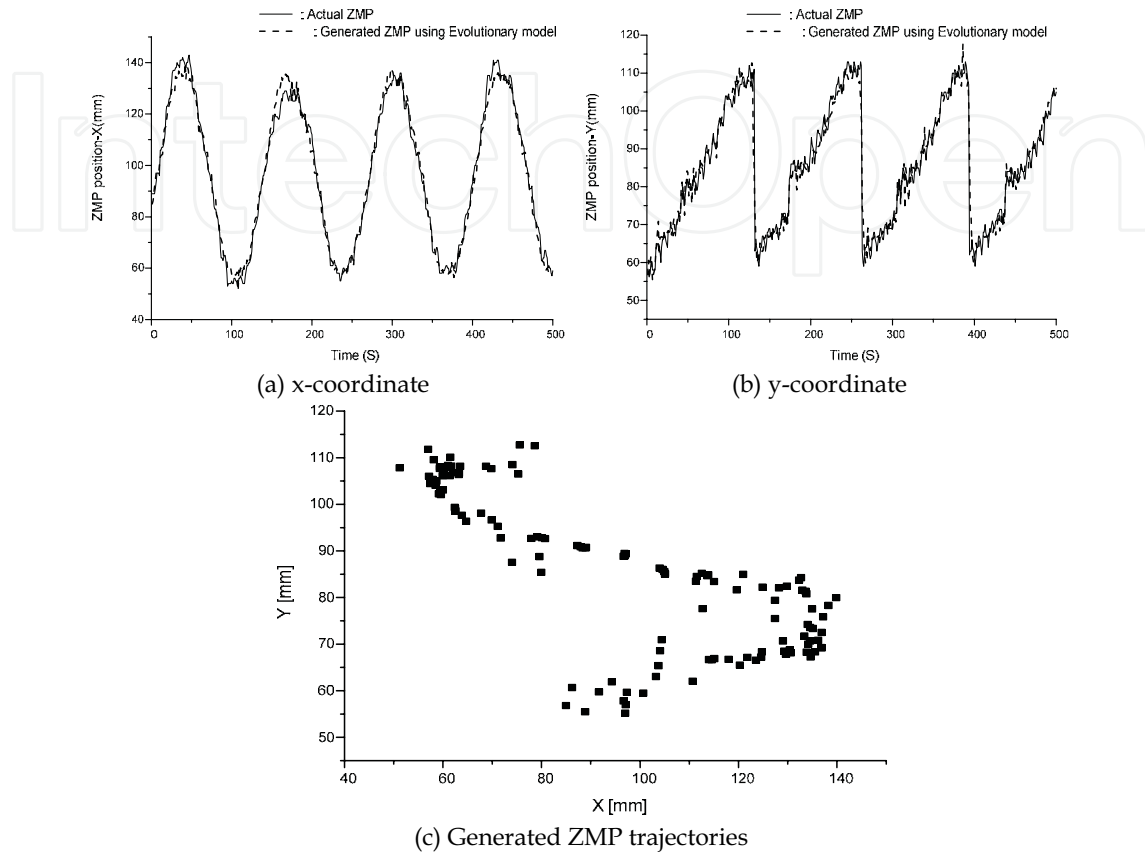
(a) x-coordinate

(b) y-coordinate

(c) Generated ZMP trajectories

Fig. 20. Generated ZMP positions and corresponding ZMP trajectories (10°).

6. Acknowledgements

7. References

[1]   Erbatur, K.; Okazaki, A.; Obiya, K.; Takahashi, T. & Kawamura, A. (2002) A study on the zero moment point measurement for biped walking robots, *7th International Workshop on Advanced Motion Control*, pp. 431-436

[2]   Vukobratovic, M.; Brovac, B.; Surla, D.; Stokic, D. (1990). *Biped Locomotion*, Springer Verlag

[3]   Takanishi, A.; Ishida, M.; Yamazaki, Y.; Kato,I. (1985). The realization of dynamic walking robot WL-10RD, *Proc. Int. Conf. on Advanced Robotics*, pp. 459-466

[4]   Hirai, K.; Hirose, M.; Haikawa, Y.; Takenaka, T. (1998). The development of Honda humanoid robot, *Proc. IEEE Int. Conf. on Robotics and Automation*, pp. 1321-1326

[5]   Park, J. H.; Rhee, Y. K. (1998). ZMP Trajectory Generation for Reduced Trunk Motions of Biped Robots. *Proc. IEEE/RSJ Int. Conf. Intelligent Robots and Systems, IROS '98,* pp. 90-95

[6]   Park, J. H.; Cho, H. C. (2000). An On-line Trajectory Modifier for the Base Link of Biped Robots to Enhance Locomotion stability, *Proc. IEEE Int. Conf. on Robotics and Automation*, pp. 3353-3358

[7]   Kim, D.; Kim, N.H.; Seo, S.J.; Park, G.T. (2005). Fuzzy Modeling of Zero Moment Point Trajectory for a Biped Walking Robot, *Lect. Notes Artif. Int.,* vol. 3214, pp. 716-722 (**BEST PAPER AWARDED PAPER**)

[8]   Kim, Dongwon; Park, Gwi-Tae. (2006). *Evolution of Inductive Self-organizing Networks*, Studies in Computational Intelligence Series: Volume 2: Engineering Evolutionary Intelligent Systems, Springer

[9]   Kim, D. W.; and Park, G. T. (2003). A Novel Design of Self-Organizing Approximator Technique: An Evolutionary Approach, *IEEE Intl. Conf. Syst., Man Cybern. 2003, pp. 4643-4648* **(BEST STUDENT PAPER COMPETITION FINALIST AWARDED PAPER)**

[10]   Takagi, H.; Hayashi, I. (1991). NN-driven fuzzy reasoning, *Int. J. Approx. Reasoning*, Vol. 5, No. 3, pp. 191-212

[11]   Sugeno, M.; Kang, G. T. (1988). Structure identification of fuzzy model, *Fuzzy Sets Syst.*, Vol. 28, pp. 15-33

[12]   Kondo, T. (1986). Revised GMDH algorithm estimating degree of the complete polynomial, *Tran. Soc. Instrum. Control Eng.*, Vol. 22, No. 9, pp. 928-934 (in Japanese)

[13]   Wu, S.; Er, M.J.; Gao, Y. (2001). A Fast Approach for Automatic Generation of Fuzzy Rules by Generalized Dynamic Fuzzy Neural Networks, *IEEE Trans. Fuzzy Syst.*, Vol. 9, No. 4, pp. 578-594

[14]   Horikawa, S. I.; Furuhashi, T.; Uchikawa, Y. (1992). On Fuzzy modeling Using Fuzzy Neural Networks with the Back-Propagation Algorithm, *IEEE Trans. Neural Netw.*, Vol. 3, No. 5, pp. 801-806

Humanoid Robots: New Developments

Edited by Armando Carlos de Pina Filho

ISBN 978-3-902613-00-4

Hard cover, 582 pages

Publisher I-Tech Education and Publishing

Published online 01, June, 2007

Published in print edition June, 2007

For many years, the human being has been trying, in all ways, to recreate the complex mechanisms that form the human body. Such task is extremely complicated and the results are not totally satisfactory. However, with increasing technological advances based on theoretical and experimental researches, man gets, in a way, to copy or to imitate some systems of the human body. These researches not only intended to create humanoid robots, great part of them constituting autonomous systems, but also, in some way, to offer a higher knowledge of the systems that form the human body, objectifying possible applications in the technology of rehabilitation of human beings, gathering in a whole studies related not only to Robotics, but also to Biomechanics, Biomimmetics, Cybernetics, among other areas. This book presents a series of researches inspired by this ideal, carried through by various researchers worldwide, looking for to analyze and to discuss diverse subjects related to humanoid robots. The presented contributions explore aspects about robotic hands, learning, language, vision and locomotion.

How to reference

In order to correctly reference this scholarly work, feel free to copy and paste the following:

Dongwon Kim and Gwi-Tae Park (2007). Advanced Humanoid Robot Based on the Evolutionary Inductive Self-Organizing Network, Humanoid Robots: New Developments, Armando Carlos de Pina Filho (Ed.), ISBN: 978-3-902613-00-4, InTech, Available from:
http://www.intechopen.com/books/humanoid_robots_new_developments/advanced_humanoid_robot_based_on_the_evolutionary_inductive_self-organizing_network